Manuscript submitted to: Volume 2, Issue 2, 86-96.

AIMS Materials Science DOI: 10.3934/matersci.2015.2.86

Received date 30 March 2015, Accepted date 10 May 2015, Published date 19 May 2015

Research article

Characterisation of $Ga_{1-x}In_xSb$ quantum wells (x~0.3) grown on GaAs using AlGaSb interface misfit buffer

Jonathan P. Hayton*, Andrew R.J. Marshall, Michael D. Thompson, and Anthony Krier

Physics Department, Lancaster University, Lancaster, LA1 4YB, UK

* **Correspondence:** Email: j.hayton1@lancaster.ac.uk; Tel: +44-(0)1524-595750.

Abstract: GaInSb multiple quantum wells (MQW) grown on GaAs using an AlGaSb interface misfit (IMF) metamorphic buffer layer technique exhibit superior infrared photoluminescence (PL) at room temperature compared with MQW grown directly on GaSb. PL emission was obtained in the range from 1.7 µm (4 K) to 1.9 µm (300 K) from $Ga_{1-x}In_xSb$ samples containing five compressively strained QW with In content x~0.3. Structural and optical characterisation confirms that the AlGaSb IMF growth technique is promising for the development of photonic devices operating at extended wavelengths based on GaAs substrates.

Keywords: photoluminescence; IMF; Interfacial Misfit Array; GaSb; AlGaSb; InGaSb; Quantum Well; MQW

1. Introduction

Antimonide based quantum wells and nanostructures continue to attract considerable interest due to their potential for accessing technologically important applications in the spectral range beyond 1.5 µm. In particular GaInSb/GaSb offers a route towards the development of sources and detectors for use in remote gas sensing instrumentation, medical diagnostics and night vision technologies [1,2]. GaSb-based diode lasers, LEDs and photodetectors have been developed with excellent performance characteristics operating at many of the key wavelengths including methane [3], CO_2 [4] and CO. However, the lack of semi-insulating GaSb substrates precludes the

development of monolithic focal plane arrays and more complex devices, while the relatively high cost of GaSb wafers makes large volume applications cost-sensitive. Consequently, it is worthwhile investigating alternative growth methods for GaInSb based device structures on inexpensive GaAs substrates, which are readily available as semi-insulating wafers and for which there exists a mature processing technology. Recently, the growth of GaSb on GaAs has been successfully demonstrated using the interface misfit (IMF) [5,6,7] technique, which accommodates the lattice mismatch by forming lateral misfit dislocations along the GaSb-GaAs interface rather than threading dislocations in the GaSb bulk. However, samples grown using this molecular beam epitaxy (MBE) technique have shown reduced optical quality compared with homoepitaxial material since not all the dislocations are accommodated at the heterointerface and the remaining threading dislocations can still be problematic. In the present work we report on the MBE growth of AlGaSb as a ternary IMF metamorphic buffer layer on GaAs and study the properties of GaInSb quantum wells grown on this novel relaxed quasi substrate. AlGaSb conveniently provides substantial offsets in both the conduction and valence bands and results in improved photoluminescence efficiency from AlGaSb/InGaSb MQWs.

2. Materials and Method

The $Ga_{1-x}In_xSb$ MQW structures were grown on a (100) orientated n-GaSb substrate, or in the case of the IMF samples a (100) n-GaAs substrate, by solid source MBE using a VG-V80H reactor fitted with a Sb valved cracker cell. The GaSb MQW sample (QA216) in Figure 1(a) was grown at a substrate temperature of 510 °C using growth rates of 0.65 ML/s for the GaSb and 1 ML/s for the $Ga_{1-x}In_xSb$ QW respectively. Once a buffer layer of GaSb was grown, GaInSb QWs with 50 nm GaSb barriers were repeated 5 times. The GaSb IMF (QA276) in Figure 1(b) was grown using these conditions with the GaSb IMF growth based on the method used previously for GaSb IMF on GaAs [8]. The ternary AlGaSb IMF sample (QJ410), in Figure 1(c) was grown in a similar manner with a 1μm AlGaSb buffer layer. For the AlGaSb MQW sample a growth rate of 0.46 ML/s with a substrate temperature of 515 °C was used. After the IMF growth a 1 μm buffer had been grown, 5x InGaSb QWs with 50 nm $Al_{0.53}Ga_{0.47}Sb$ barriers were grown before finally capping with 100 nm of AlGaSb. Details of the resulting structures are given in Table 1.

The structural properties of the resulting samples were studied using high resolution x-ray diffraction (XRD) and transmission electron microscopy (TEM), to obtain information about dislocations, In content, thickness and perfection of the MQWs. In order to probe the optical properties of the samples, PL spectroscopy (4-300 K) was carried out using a continuous flow helium cryostat (Oxford Instruments Optistat). Excitation at 514 nm was provided by an Ar^+ ion laser giving an adjustable power density of 0.4 to 10 Wcm^{-2} at the sample surface. The PL emission was detected and analysed using a Bentham M300 monochromator having a grating blazed at 3.5 μm, with a 77 K InSb photodiode detector and lock-in amplifier.

Table 1. A summary of the properties of the different samples under investigation and the resulting measured parameters.

			QA216	QA276	QJ410
Buffer layer			GaSb	GaSb IMF	AlGaSb IMF
QW thickness (L_z)/ nm			4±1	4±1	7±4
QW In content (%)			34	32	28
Strain (%)			2.1	2.0	1.4
PL peak	Wavelength (μm)		1.77	1.77	1.70
	Energy (eV)		0.699	0.703	0.728
Relative PL intensity (10 K)			1	0.025	0.66
FWHM (meV) at 4 K			15.4	16.7	20.5
Confinement energy (meV)		e^-	49	48	506
		h^+	98	98	345
Z parameter	4K		1.9	1.2	1.8
	225K		2.2	-	2.3

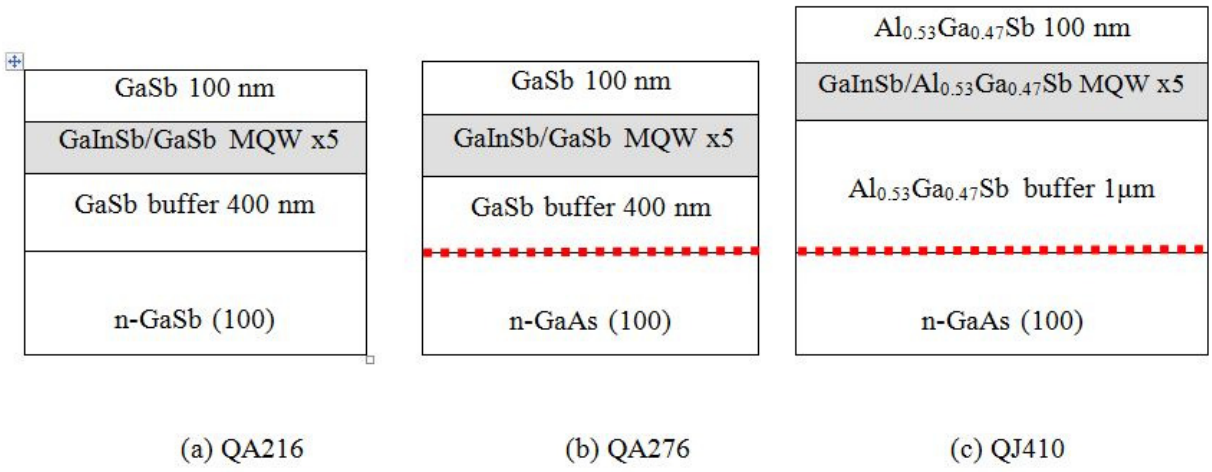

Figure 1. A schematic diagram showing the different structures studied. (a) QA216: InGaSb/GaSb MQW grown homoepitaxially on GaSb substrate; (b) QA276: the same MQW structure as in (a) but grown on GaAs using the GaSb IMF buffer layer; (c) QJ410: a ternary $Al_{0.53}Ga_{0.47}Sb$ layer is used instead of GaSb for the IMF and also in the MQW barriers for additional confinement. (The IMF is represented with a red dashed line).

3. Results and Discussion

The high resolution XRD spectra obtained from each of the samples is shown in Figure 2. Sample (QA216) which was grown homoepitaxially on GaSb, has clearly defined satellite peaks with a full width half maximum (FWHM) of 78 arcsecs and a GaSb peak with FWHM of 27 arcsecs, indicating high crystalline quality. For sample (QA276) the satellite peaks are less distinct, being reduced in intensity with a FWHM of ~200 arcsecs, while the peak from the GaSb grown IMF layer is broadened with a FWHM of ~220 arcsecs; although this behaviour is consistent with the broadening of quasi substrate peaks seen in other IMF samples [9].

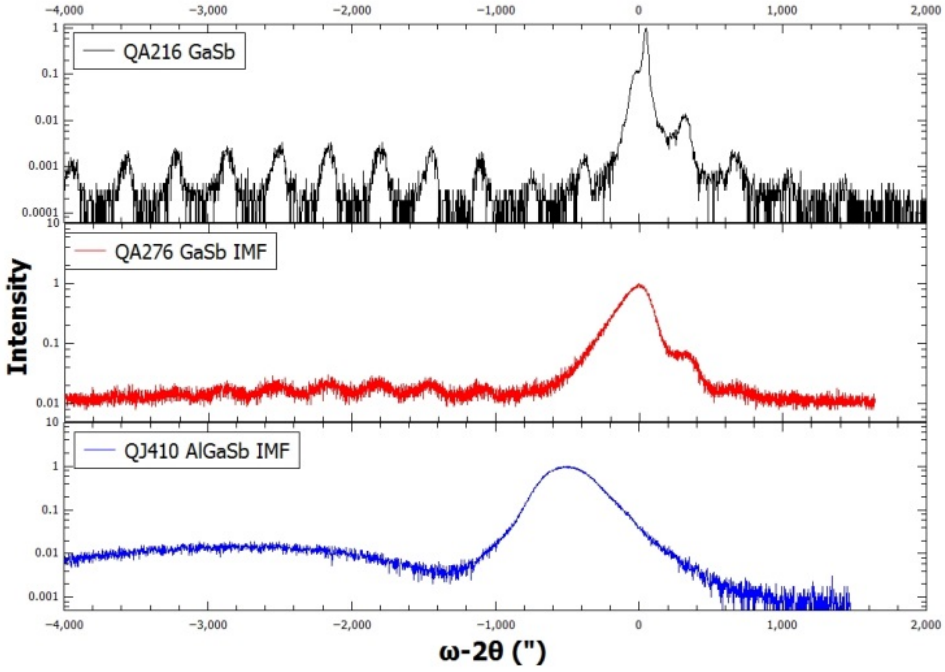

Figure 2. High resolution x-ray diffraction (XRD) spectra obtained from each of the samples. (a) QA216 MQW on GaAs; (b) QA276 MQW on GaSb IMF grown on GaAs and (c) QJ410 MQW with AlGaSb barriers grown on ternary AlGaSb IMF on GaAs.

The XRD spectrum of QJ410 with the ternary AlGaSb IMF metamorphic buffer structure shown in Figure 1(c) has no observable satellite peaks and a rather broad AlGaSb "quasi-substrate" broad band with a FWHM of 473 arcsecs. The lack of satellite peaks is normally indicative of a mixed composition layer, or a structure which contains several different lattice parameters. To help elucidate this, TEM images of this sample are shown at different magnifications in Figure 3. The ternary IMF dislocation array is clearly evident at the AlGaSb-GaAs interface in Figure 3(a) and the MQW are shown in the higher magnification image of Figure 3(b). Figure 3(c) shows that the overall

quality of the metamorphic buffer using the AlGaSb is high with relatively few threading dislocations. Abrupt thickness fluctuations in the QWs are clearly observable under high magnification in Figure 3(b). The target QW thickness was 6 nm but the actual QWs vary in a step-like fashion with thickness from 7 nm to 12 nm across the sample, which is sufficient to prevent the observation of the satellite peaks in the XRD spectrum. The appearance of these abrupt thickness variations is reminiscent of the early stages of quantum dot formation as the strain limit is approached but may also be related to the growth temperature, since 515 °C was used throughout to avoid the growth interrupt normally employed to grow InGaSb and AlGaSb layers at their respective optimum temperatures, (480 °C and 515 °C respectively).

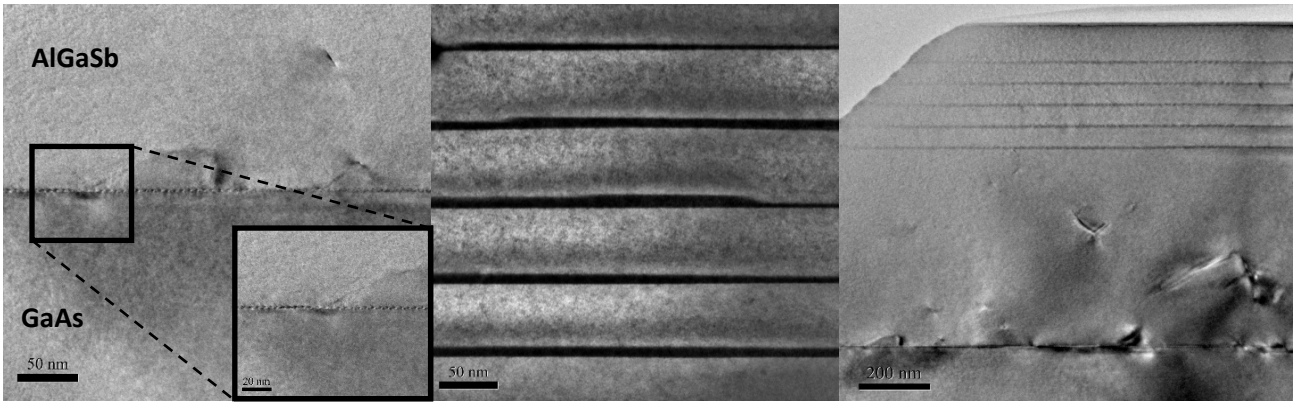

Figure 3. Cross-sectional TEM images of the $Al_{0.53}Ga_{0.47}Sb$ IMF MQW sample; (a) an image of the IMF AlGaSb-GaAs interface showing the misfit dislocation array; (b) a high resolution image of the MQW region, showing the non-uniform thickness of the InGaSb QWs; (c) a low magnification image showing the buffer layer which contains only a few threading dislocations.

A comparison of the 4 K PL spectra from each of the MQW samples is shown in Figure 4. The relative intensities, peak energy and FWHM are given in Table 1. The peak energies are in reasonable agreement with the calculated values obtained using a Schrödinger solver for a finite quantum well within the effective mass approximation. The corresponding confinement energies for electrons and holes are given in Table 1. The calculations are based on the indium compositions and QW thickness values obtained from the growth parameters, XRD measurements and TEM images. Although the MQW in samples QA216 and QA276 have nominally the same structure, the QA276 GaSb IMF sample has a slightly higher peak energy of 0.703 eV compared with 0.699 eV due to a decrease in Indium content of 1.7% which originates from a change in growth rate when growing on the IMF buffer. Meanwhile, in sample QJ410 the higher band offset provided by the $Al_{0.53}Ga_{0.47}Sb$ produces higher confinement and consequently the peak energy is further increased to 0.729eV.

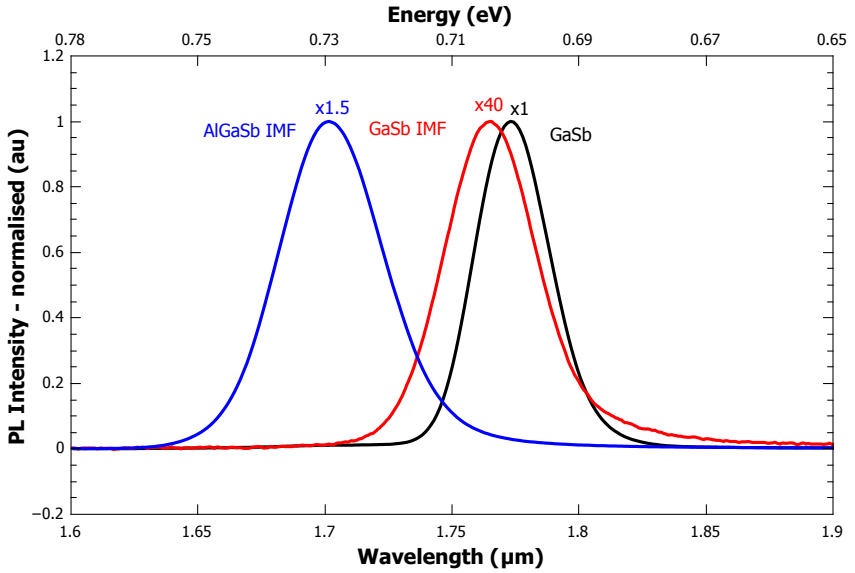

(a)

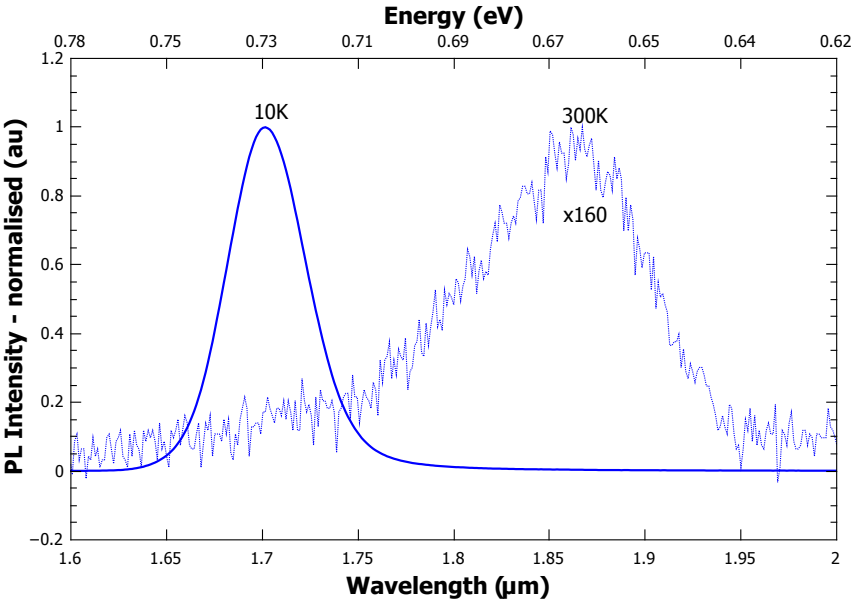

(b)

Figure 4. (a) The normalised photoluminescence at 10 K from each of the MQW samples. The FWHM were measured as 15.4, 16.7 and 20.5 meV for GaSb, GaSb IMF and AlGaSb respectively; (b) The 10 K and 300 K PL obtained from sample QJ410.

The FWHM of the samples at 4 K (Table 1) compare favourably with samples grown previously both on native GaSb substrates and on Si [10]. The temperature dependent PL of QJ410

exhibits emission up to room temperature due to the stronger carrier confinement provided by the AlGaSb barriers. The FWHM increases to 39.5 meV as shown in Figure 4(b), and an exponential tail is observed which extends up to higher energy which is associated with band filling and thermal broadening in the QWs.

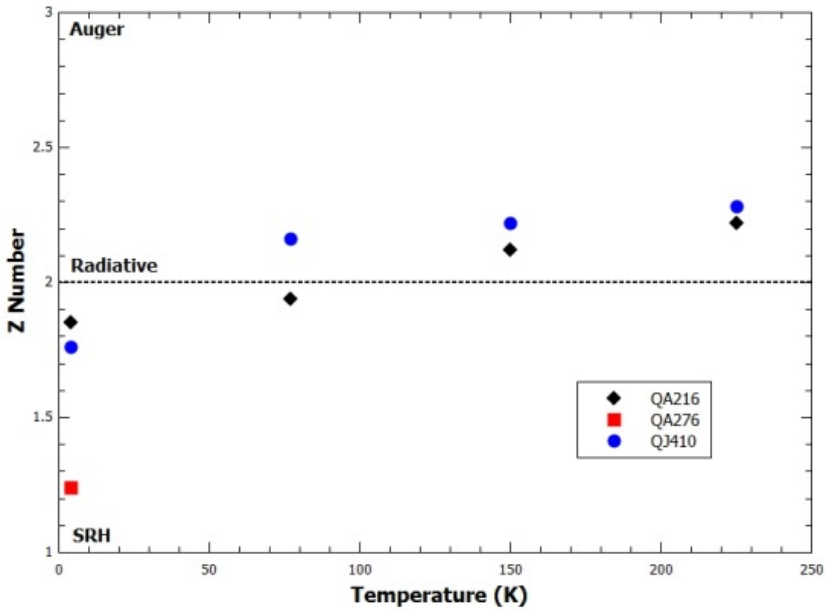

Figure 5. The temperature dependence of the Z value for each of the MQW samples; QA216—black solid diamonds, QJ410—solid blue points, QA276—solid red squares.

The power dependence of the PL emission from each of the samples was also measured to determine the dominant recombination process based on the PL intensity (L) vs pump power (I) expression; $L \propto I^{\frac{z}{2}}$ where the exponent Z = 1 corresponds to Shockley-Read-Hall (SRH), Z = 2 corresponds to radiative recombination and Z = 3 corresponds to non-radiative Auger recombination respectively [11]. The corresponding Z parameter are given in Table 1 from which we observe that recombination is predominantly radiative in these samples except for QA276 where SRH recombination is more significant at 10 K. These values are also plotted in Figure 5 showing the much lower value for QA276 which is attributed to defects in the lattice structure whilst showing a nominally constant radiative-dominated process in both QA216 and QJ410. Due to the limitations of this method, differences in Z paramter of ~0.1 can be considered negligible due to the assumptions in the model including the need for a constant number of carriers.

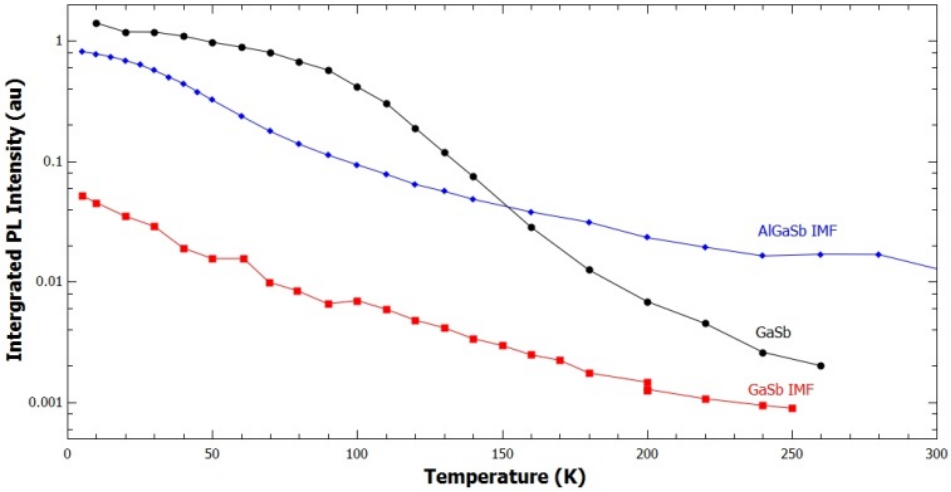

Figure 6. The temperature dependence of the integrated PL emission intensity for each of the MQW samples; QA216—black solid points, QJ410—solid blue diamonds, QA276—solid red squares

The temperature dependence of the integrated PL emission intensity is shown in Figure 6. The high initial intensity of QA216 at 10 K is attributed to better crystalline perfection. The recombination is predominantly radiative and the thermal quenching is determined by limited carrier (electron) confinement in the MQWs. Sample QA276 quenches at about the same rate as QJ410 but has the lowest 4 K PL intensity which is as expected from the increased threading dislocation density originating from the heteroepitaxial growth mediated by the IMF buffer layer. By comparison the 4 K PL intensity of the AlGaSb ternary IMF sample (QJ410) is about one order higher over the entire temperature range. The increased confinement arising from the AlGaSb barriers helps to maintain PL emission up to room temperature compared to the other two samples which are quenched above ~250 K. This is also supported by the nominally equal recombination processes in QA216 and QJ410 but weaker emission from the smaller barriers of QA216. Both IMF based samples (QA276 and QJ410) are also more susceptible to carrier recombination in the barriers due to the higher levels of threading dislocations and structure defects compared with the homoepitaxial sample QA216.

4. Conclusion

In summary, we have reported the MBE growth of strained InGaSb/(Al)GaSb MQW structures containing ~30% In on GaSb and GaAs substrates using IMF buffers of both GaSb and ternary AlGaSb. The structural properties of the different samples and the effect on the PL emission efficiency and thermal quenching were compared. The structural perfection and crystallinity of the homoepitaxial MQW was found to be superior and the thermal quenching in this case is determined mainly by the electron-hole confinement in the QW. Transferring this structure directly onto GaAs

using a GaSb IMF approach resulted in inferior PL emission intensity at 4 K and thermal quenching of the emission above 250 K, which we attributed to non-radiative SRH recombination within the GaSb barriers. By comparison, it has been shown that when a ternary AlGaSb IMF is used instead, the 4 K PL intensity is considerably recovered and the PL emission persists up to room temperature, due to the improved crystallinity of the ternary IMF and the additional carrier confinement for both electrons and holes arising from the AlGaSb barriers. In each case the PL emission peaks were reconciled with the calculated values. Although further optimisation is required to improve the thickness uniformity of the InGaSb MQW, we have shown that $Al_{0.53}Ga_{0.47}Sb/Ga_{0.7}In_{0.3}Sb$ MQWs grown on GaAs using a ternary $Al_{0.53}Ga_{0.47}Sb$ IMF buffer layer can provide a viable alternative to growth on GaSb substrates to access longer wavelength applications since it facilitates the use of both inexpensive and semi-insulating substrates.

Acknowledgements

This work was supported by The Centre for Global Eco-Innovation, Oxley Developments Ltd & European Regional Development Fund 2007-13. Thanks are also given to Dr Richard Beanland of Warwick University for the TEM images.

Conflict of Interest

All Authors declare no conflicts of interest in this paper

References

1. Pascal-Delannoy F, Bouganot J, Allogho G, et al. (1992) MOVPE grown Ga0.6In0.4Sb photodiodes for 2.55um detection. *Electron Lett* 28: 531–532.
2. Bertru N, Baranov A, Cuminal Y, et al. (1998) Long-wavelength (Ga, In)Sb/GaSb strained quantum well lasers grown by molecular beam epitaxy. *Semicond Sci Technol* 13: 936.
3. Krier A, Sherstnev V (2000) Powerful interface light emitting diodes for methane gas detection. *J Phys D Appl Phys* 33: 101.
4. Refaat T, Abedin M, Koch G, et al. (2003) Infrared detector characterization for CO_2 DIAL measurement. in Proc. SPIE 5154, Lidar Remote Sensing for Environmental Monitoring IV, San Diego, California, USA.
5. Rotter TJ, Tatebayashi J, Senanayake P, et al. (2009) Continuous-Wave, Room-Temperature Operation of 2-μm Sb-Based Optically-Pumped Vertical-External-Cavity Surface-Emitting Laser Monolithically Grown on GaAs Substrates. *Appl Phys Express* 2: 112102.
6. Demeo D, Shemelya C, Downs C, et al. (2014) GaSb Thermophotovoltaic Cells Grown on GaAs Substrate Using the Interfacial Misfit Array Method. *J Electronic Mater* 43: 902–908.

7. Craig A, Marshall A, Tian Z, et al. (2013) Mid-infrared InAs0.79Sb0.21-based nBn photodetectors with Al0.9Ga0.2As0.1Sb0.9 barrier layers, and comparisons with InAs0.87Sb0.13 p-i-n diodes, both grown on GaAs using interfacial misfit arrays. *Appl Phys Lett* 103: 253502.
8. Huang S, Balakrishnan G, Huffaker D (2009) Interfacial misfit array formation for GaSb growth on GaAs. *J Appl Phys* 105: 103104.
9. Reyner C, Wang J, Nunna K, et al. (2011) Characterization of GaSb/GaAs interfacial misfit arrays using x-ray diffraction. *Appl Phys Lett* 99: 231906.
10. Akahane K, Yamamoto N, Gozu S, et al. (2006) (In)GaSb/AlGaSb quantum wells grown on Si substrates. *Thin Solid Films* 515: 4467–4470.
11. Jin S, Sweeney S (2003) High-Pressure Studies of Recombination Mechanisms in 1.3um GaInNAs Quantum-Well Lasers. *IEEE J Sel Top Quantum Electron* 9: 1196.